Improved Prediction of Wave Excitation Forces Using Small-Body Based Correction

Adi Kurniawan, Hugh Wolgamot, Jana Orszaghova
School of Earth and Oceans, The University of Western Australia, Australia
adi.kurniawan@uwa.edu.au

1 LINEAR SMALL-BODY APPROXIMATION

The small-body approximation of the wave excitation force, as we know it from linear theory (see, e.g., [1]), has the form

$$F_{e,i} = \rho \overline{\forall} a_{0,i} + \sum_{j=1}^{3} A_{ij} a_{0,j} + \rho g \overline{S}_w \eta_0 \delta_{3i}, \tag{1}$$

where $\overline{\forall}$ is the displaced volume of the body, A_{ij} is the added mass, $a_{0,i}$ is the ith component of the fluid acceleration (due to the unidisturbed incident wave) at a suitable reference point, $\overline{S}_w$ is the water plane area, η_0 is the incident free-surface elevation, ρ is the fluid density, g is the acceleration due to gravity, and δ_{ij} is the Kronecker delta. The first and third terms are the small-body approximation of the Froude-Krylov force, while the second term is the small-body approximation of the diffracted force. The displaced volume and water plane area are taken at the body's mean position.

2 GENERALISATION OF THE SMALL-BODY APPROXIMATION

The small-body approximation (1) has a simple form. Can we extend its range of validity to cases where the wave steepness or the body size may not be small? The simplest improvement we can try is to replace mean quantities in (1) with time-dependent quantities such that

$$F_{e,i} = \rho \forall(\eta_0(t)) a_{0,i} + \sum_{j=1}^{3} A_{ij} a_{0,j} + \rho g \left(\forall(\eta_0(t)) - \overline{\forall} \right) \delta_{3i}, \tag{2}$$

where $\forall(\eta_0(t))$ is now the instantaneous displaced volume. In effect, this removes the linearity assumption to some extent but does not remove the small-body assumption. Rather than using (2) directly, we propose a correction to the linear excitation force, based on (2). This will be illustrated with the simplest case of regular wave excitation. But first, we need to show if approximation (2) is plausible beyond linear theory.

With ϕ being the velocity potential and $\mathbf{v} = \nabla\phi$ the fluid velocity, the dynamic pressure follows from Bernoulli's equation. The excitation force on the body is obtained by integrating this pressure over the wetted body surface S_b. While the body itself is fixed, S_b is time-varying due to the varying free surface η. Decomposing the velocity potential ϕ into incident and diffracted potentials ϕ_0 and ϕ_d, we have

$$\mathbf{F}_e = \rho \iint_{S_b} \left(\frac{\partial \phi_0}{\partial t} + \frac{v_0^2}{2} \right) \mathbf{n}\, \mathrm{d}S + \rho \iint_{S_b} \mathbf{v}_0 \cdot \mathbf{v}_d\, \mathbf{n}\, \mathrm{d}S + \rho \iint_{S_b} \left(\frac{\partial \phi_d}{\partial t} + \frac{v_d^2}{2} \right) \mathbf{n}\, \mathrm{d}S, \tag{3}$$

with the unit normal vector $\mathbf{n}$ defined to be pointing out of the body.

Considering first the Froude-Krylov part—the first integral in (3)—we can write

$$\mathbf{F}_{\mathrm{FK}} = \rho \oiint_{S_b+S_w} \frac{\partial \phi_0}{\partial t} \mathbf{n}\, \mathrm{d}S + \rho \oiint_{S_b+S_w} \frac{v_0^2}{2} \mathbf{n}\, \mathrm{d}S + \rho g \iint_{S_w} \eta_0\, \mathbf{n}\, \mathrm{d}S, \tag{4}$$

where S_w is the portion of the free surface bounded by the body. The last term arises from the dynamic free-surface boundary condition. If we assume that the body is small, i.e., v_0 is constant over the body, then the second integral in (4) vanishes. Applying the divergence theorem to the first integral gives

$$\mathbf{F}_{\mathrm{FK}} = \rho \forall(\eta_0(t))\, \mathbf{a}_0(t) + \rho g \iint_{S_w} \eta_0\, \mathbf{n}\, \mathrm{d}S, \tag{5}$$

where $\forall(\eta_0(t))$ is the instantaneous displaced volume of the body and $\mathbf{a}_0(t)$ is the acceleration of the fluid due to the incident wave. For the last integral, in the linear case, S_w is equal to $\overline{S}_w$, which lies on the horizontal plane, so only the vertical component is nonzero. In the nonlinear case, however, S_w is not necessarily horizontal and so in general there is a nonzero horizontal component arising from this term in addition to a vertical component.

The first term in the diffracted part—the third integral in (3)—can be expressed in terms of the radiation potentials by using the Haskind relation. An amenable treatment of this integral seems possible only through linear approximation, i.e., by taking S_b as the mean wetted body surface, as in the linear case. The small-body approximation then gives, for the ith component,

$$F_{d,i} \approx \sum_{j=1}^{3} A_{ij} a_{0,j}(t) + \rho \iint_{S_b} \frac{v_d^2}{2} n_i \,\mathrm{d}S, \tag{6}$$

after neglecting the radiation damping part and keeping only the added mass A_{ij}, since the radiation impedance of a small body is usually dominated by the imaginary part.

The second integral in (6) can be combined with the second integral in (3) and written as

$$\rho \oiint_{S_b+S_w} \frac{1}{2} |\mathbf{v}_0 + \mathbf{v}_d|^2 \,\mathbf{n} \,\mathrm{d}S - \rho \iint_{S_w} \frac{1}{2} \left(v_d^2 + 2\mathbf{v}_0 \cdot \mathbf{v}_d\right) \mathbf{n} \,\mathrm{d}S. \tag{7}$$

Assuming a small body, the first integral is zero. The second integral is an integral over S_w, having the same form as the last integral in (4).

Thus far we have shown that the first terms of (5) and (6) are the first and second terms of (2). The remaining term, based on the preceding derivation, is

$$\rho g \iint_{S_w} \eta_0 \,\mathbf{n} \,\mathrm{d}S - \rho \iint_{S_w} \frac{1}{2} \left(v_d^2 + 2\mathbf{v}_0 \cdot \mathbf{v}_d\right) \mathbf{n} \,\mathrm{d}S, \tag{8}$$

which, alternatively, may be written as

$$\rho g \iint_{S_w} (\eta_0 + \eta_d) \,\mathbf{n} \,\mathrm{d}S + \rho \iint_{S_w} \frac{\partial \phi_d}{\partial t} \,\mathbf{n} \,\mathrm{d}S \tag{9}$$

by virtue of the dynamic free-surface boundary condition. While this is not quite the same as the last term in (2), it may explain why $\rho g \left(\forall(\eta_0(t)) - \overline{\forall}\right) \delta_{3i}$ gives a better prediction, as we have found, than $\rho g S_w(\eta_0(t))\, \eta_0(t)\, \delta_{3i}$, which one obtains from (1) if one simply replaces the mean quantities by the time-varying ones. Therefore, we adopt (2) as the basis of our model.

3 SMALL-BODY BASED CORRECTION

Having shown that (2) is a reasonable form to use beyond the linear case, we will now describe our correction. Assuming that the linear force $(\mathbf{F}_e)_{\mathrm{lin}}$ is known, we seek a model of the form

$$F_{e,i}(t) = \mathrm{Re}\left\{ (\hat{F}_{e,i})_{\mathrm{lin}} \sum_{n=1}^{N} \frac{(\hat{F}_{e,i,\mathrm{SB}})_n}{(\hat{F}_{e,i,\mathrm{SB}})_{\mathrm{lin}}} \mathrm{e}^{\mathrm{i}n\omega t} + |(\hat{F}_{e,i})_{\mathrm{lin}}| \frac{(\hat{F}_{e,i,\mathrm{SB}})_0}{|(\hat{F}_{e,i,\mathrm{SB}})_{\mathrm{lin}}|} \right\}, \tag{10}$$

where $\hat{}$ denotes the complex amplitude, n denotes the nth harmonic, and N is the highest harmonic to be included in the model. Here, $(F_{e,i,\mathrm{SB}})_{\mathrm{lin}}$ is the linear small-body approximation (1), and $(F_{e,i,\mathrm{SB}})_n$ is the nth harmonic of (2). The 0th harmonic (the mean component) is separated from the main sum because the mean is indifferent to a phase shift. This model effectively assumes that the proportions of the higher harmonic forces relative to the linear ones are maintained regardless of the size of the body. The form (10) applies to regular incident waves of frequency ω. It might be possible to formulate a more general form applicable to irregular waves.

4 EXAMPLE

As an example, we compare our predictions with high-precision measurements reported in [2]. A half-submerged sphere of radius $r = 0.15$ m is fixed in water of depth $h = 0.9$ m and subjected to regular waves. We select three cases with wave heights and periods given in Table 1. Case R12 is the most severe wave in terms of its steepness and height relative to the body size, while R05 is the shortest wave relative to the body.

Table 1: Regular wave conditions.

Case	wave height H [m]	wave period T [s]	$\frac{H}{\lambda}$	$\frac{2r}{\lambda}$	$\frac{H}{2r}$
R01	0.0181	1.14	0.009	0.149	0.060
R05	0.0561	0.88	0.046	0.248	0.187
R12	0.2611	1.42	0.087	0.100	0.870

For a given wave height and period, the incident free-surface elevation $\eta_0(t)$ in (2) is obtained from stream function theory [3] as implemented in the CN-Stream libraries [4], while the linear form is used in (1). For simplicity, we assume $\eta_0(t)$ to always have a horizontal profile within the body. The accelerations in (1) and (2) are both calculated at the mean centroid of the body. Again, for simplicity, the accelerations in (2) are calculated as in the linear case, but with the linear $\eta_0(t)$ replaced with $\eta_0(t)$ obtained from stream function theory. In addition, the added masses in (1) and (2) are identical and calculated assuming a perfect hemisphere as the wetted body. The linear excitation forces and added masses are obtained from HydroStar [5].

Figure 1 compares the predicted excitation forces with the measurements. The measurements have been digitised from [2]. However, no data were reported for R05. We see that the crest of the surge force is amplified with wave steepness, while the heave force is reduced at the peak. The applied correction does well in capturing these features even for the steepest case R12, whereas linear theory is clearly inadequate. Good prediction is obtained particularly for the heave force, whereas certain features of the surge force are not as well captured, notably the flat region around a zero upcrossing. The ratios of the predicted harmonics to the linear amplitude are shown in Fig. 2 for the three wave conditions. Perhaps the most striking observation is the significant reduction of the first harmonic excitation force in heave for the steepest condition R12. The amplitude of the first harmonic force is reduced to 67% of the linear amplitude. If the sphere is a heaving wave energy absorber, this implies that it would absorb less than half the power predicted using linear theory from the same wave. The ratio of the first harmonic heave force to the linear amplitude for this body geometry is always less than one.

These results indicate how much more nonlinear the excitation forces may be than the incident waves, due to the interactions of the wave with the body. Figure 2 appears to suggest that a half-submerged sphere would be a better wave energy absorber if it operates in surge rather than heave.

REFERENCES

[1] Newman, J. N. 2017. *Marine Hydrodynamics*. The MIT Press, Cambridge, MA. 40th Anniversary Edition.

[2] Andersen, J., and Kramer, M. B. Wave excitation tests on a fixed sphere: Comparison of physical wave basin setups. In *Proceedings of the 15th European Wave and Tidal Energy Conference* (Sep 2023).

[3] Rienecker, M. M., and Fenton, J. D. 1981. *A Fourier approximation method for steady water waves*. *Journal of Fluid Mechanics 104*, 119–137.

[4] Ducrozet, G., Bouscasse, B., Gouin, M., Ferrant, P., and Bonnefoy, F. CN-Stream: Open-source library for nonlinear regular waves using stream function theory, 2019.

[5] Veritas, B. *HydroStar for Experts - User Manual*. Bureau Veritas, Neuilly-Sur-Seine, 4 2021. v8.10.

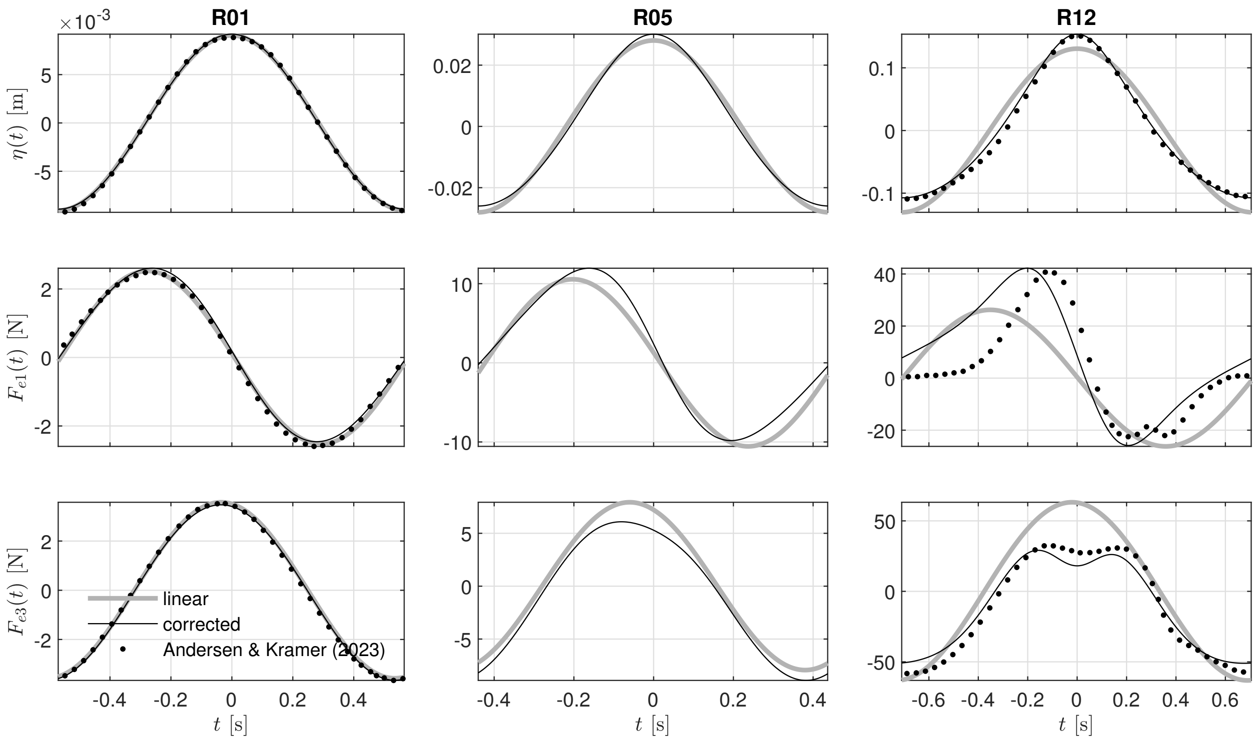

Figure 1: Comparison of the free-surface elevation, excitation force in surge, and excitation force in heave from linear theory, the corrected version, and measurements.

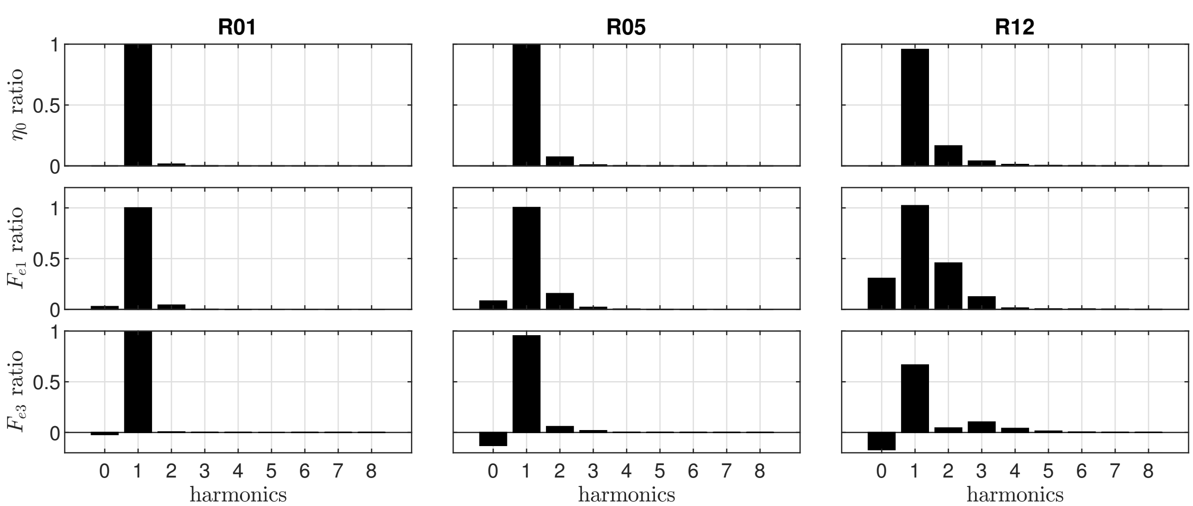

Figure 2: Ratios of the harmonics to the linear: incident wave (top), surge excitation force (middle), heave excitation force (bottom).